Int J Clin Exp Med 2025;18(7):154-171
www.ijcem.com /ISSN:1940-5901/IJCEM0162932

*Original Article*

# Bidirectional regulatory effects of Panax notoginseng saponins on aldose reductase: insights from molecular docking and *in vitro* experiments

Wei-Jie Jian[1], Si Chen[1], Ming-Xing Yue[1], Wen-Ting Fei[1*], Jian-Mei Huang[2*], Guan-Chao Du[3]

*[1]School of Bioengineering, Beijing Polytechnic University, Beijing, China; [2]School of Chinese Materia Medica, Beijing University of Chinese Medicine, Beijing, China; [3]Department of Andrology, Xiyuan Hospital, China Academy of Chinese Medical Sciences, Beijing, China. [*]Equal contributors.*

Received December 25, 2024; Accepted June 9, 2025; Epub July 15, 2025; Published July 30, 2025

**Abstract:** Objective: This study was conducted to screen different components of Panax notoginseng saponins, evaluate their activity and effects on aldose reductase by molecular docking analysis, and investigate their effects on lens aldose reductase (LAR) and kidney aldose reductase (KAR) *in vitro*, aiming to provide a reference for screening aldose reductase inhibitors (ARIs). Methods: The prototypical and metabolic components of Panax notoginseng saponins were collected. Molecular docking analysis was performed between saponins and aldose reductase. *In vitro* experiments, including aldose reductase (AR) extraction, protein content determination, enzyme activity assay optimization, and studies on the effects of saponins on LAR and KAR, were conducted. All of the data were analyzed using SPSS. Results: Saponins from Panax notoginseng had a bidirectional regulatory effect on LAR and KAR activity. The biological effects of monomeric saponin compounds on AR changed from excitatory to inhibitory with concentration changes. Different Panax notoginseng saponins demonstrated binding mode and strength differences when coincubated with AR. Conclusions: The binding of monomeric saponin components to LAR/KAR may involve a multimolecular binding mechanism. This study established a method for preparing AR crude enzymes and an enzyme activity evaluation system, providing new ideas for saponin activity research involving AR activity regulation.

**Keywords:** Panax notoginseng saponins, aldose reductase, molecular docking, diabetes retinopathy, diabetes nephropathy

## Introduction

Diabetes mellitus (DM) is a metabolic disease caused by insulin resistance or insufficient secretion that seriously impairs patients' metabolic activity. According to the World Health Organization, the number of patients with diabetes is expected to increase to 552 million by 2030 [1]. Although oral hypoglycemic agents and insulin have good and rapid effects on glucose concentrations, diabetic complications such as diabetic nephropathy and diabetic retinopathy seriously affect patients' quality of life [2, 3]. Inhibiting the polyol pathway with aldose reductase inhibitors (ARIs) is an important mechanism for targeting aldose reductase (AR) in the treatment of diabetic complications. AR catalyzes an NADPH-dependent reduction of glucose to sorbitol, and sorbitol is oxidized to fructose by NAD+-dependent sorbitol dehydrogenase under hyperglycemic conditions [4-6]. Blocking AR has beneficial effects on diabetic complications, and ARIs reduce sorbitol accumulation in the tissues of diabetic animals.

As a holistic and combinatorial approach, traditional Chinese medicine (TCM) has advantages in the treatment of diabetes [7]. Natural products have always been a unique source of potential drugs with diverse biological activities. Panax notoginseng saponins effectively prevent diabetes and its complications [8-10]. Panax notoginseng saponins are mainly classified into two types according to their structure: 20(s)-protopanaxadiol saponins and 20(s)-protopanaxtriol saponins. These compounds exhibit strong structural regularity, and the primary difference between the structures lies in

https://doi.org/10.62347/YDTS8551

the number and types of sugar substitutions in the mother nucleus. Studies on the metabolism of Panax notoginseng have demonstrated that the main metabolism mechanism of these compounds *in vivo* is a deglycosylation reaction under the action of gastric acid or the intestinal flora [11]. Ginsenoside CK and propanaxadiol are the main metabolites of protopanaxadiol-type saponins in Panax notoginseng, while protopanaxatriol is the main metabolite of protopanaxatriol-type saponins. Dalmarane tetracyclic triterpene saponins are primary physiologically active components in medicinal plants of ginseng, and Panax notoginseng is characterized by its high content of such saponins [12]. The total saponin content in Panax notoginseng root is much higher than that in ginseng and American ginseng. The content level of the main components, ginsenoside $Rg_1$ and ginsenoside $Rb_1$, exceeds 1.5%, much higher than that found in ginseng and American ginseng.

Pharmacological studies of Panax notoginseng have shown that its saponin components exert dual regulatory effects on hemostasis and blood circulation, as well as on the cardiovascular system by both inhibiting and promoting angiogenesis. Panax notoginseng also has inhibitory effects on the central nervous system, such as sedation and stabilization, and dual regulatory effects that protect the nervous system [13-16]. In addition, pharmacological and clinical studies of Panax notoginseng and its compounds have shown that it can effectively prevent and treat diabetes, a microvascular disease [17, 18]. However, whether saponins, the effective components of Panax notoginseng, can inhibit AR remains unclear.

This study aimed to screen different Panax notoginseng saponins through molecular docking analysis with AR and study the effects of Panax notoginseng saponins on lens AR and kidney AR *in vitro* to assess the active effects of Panax notoginseng saponins on AR and provide a reference for ARI screening. We first employed the molecular docking method to analyze the binding ability between saponin components and aldose-reducing sugars and then assessed the relevance between the combination method and structure. Subsequently, we used enzyme kinetics methods *in vitro* to evaluate the regulatory effect of Panax notoginseng saponins on AR activity and determine the intensity of its regulatory effect (excitation and inhibition). This study provides a basis for designing and developing ARI compounds using protopanaxadiol and protopanaxatriol saponins as the mother nucleus.

## Materials and methods

### *Screening of Panax notoginseng saponins*

The prototypical and metabolic components of Panax notoginseng saponins were collected, and saponins with different structural representations were divided according to the glycosyl substitutions in the parent nucleus.

### *Molecular docking analysis of Panax notoginseng saponins and AR*

The AR crystal structure was downloaded from the online ProteinData Bank (PDB, http://www.rcsb.org/PDB/home/home.do). AR was dehydrated and hydrogenated to complete the LOOP region and adjusted for protonation at pH 5. The binding site of the AR ligand (toristat) in the crystal structure was used as the active site of molecular docking. The 2D compound structures were converted to 3D structures using Corina, an online conversion program (http//www.molecular-networks.com). Using Discovery Studio 4.5 software (Accelrys, USA), the Libdock module was used for molecular docking to obtain the molecular docking score, the stereoscopic conformation of the compound binding to the protein crystal, and data regarding how the compound binds to the protein. The information was combined per the instructions on the website. The quality of the docking results was assessed according to the score obtained from the analysis. If the score was higher than that of the original ligand, it indicated that the conformation of the ligand-protein complex after docking was better than that of the original ligand, indicating successful docking. The higher the score was, the better the docking result.

The Calculate Interaction Energy function in the Analyze Trajectory tool in the simulation module of Discovery Studio was used to calculate the binding free energy between compounds and AR. Lower binding free energy indicated stronger binding affinity between the compounds and AR.

*In vitro experiments*

*Animals:* Animal acquisition and feeding: 30 male Sprague-Dawley (SD) rats were purchased from Biotechnology Co. Ltd., Beijing, China, Permit number: SCXK (Beijing) 2023-0071. The rats were housed in an environment with a temperature of 22 (± 2)°C and a relative humidity of 50 (± 10)%, with a 12-hour light/12-hour dark cycle and free access to food and water. All procedures were performed following approval of the Institutional Animal Care and Use Committee of Beijing University of Chinese Medicine.

Euthanasia protocol for SD rats via $CO_2$ inhalation (AVMA-Compliant): SD rats were placed in a sealed chamber, and $CO_2$ was introduced gradually at 10-30% chamber volume/min until ≥ 70% concentration was maintained for ≥ 10 minutes post-unconsciousness (confirmed by respiratory arrest).

*AR extraction and preparation of crude enzyme solution:* Referring to the AR extraction and separation method reported in reference [19], all of the steps were conducted at < 4°C. The lenses and kidneys of SD rats were harvested, and 100 mmol/L phosphate buffer (pH 6.2) was added at a 1:3 (v/w) ratio. The samples were then ground in an ice bath and centrifuged at 10,000 r/min for 20 min. The crude enzymes of lens-derived AR acid (LAR) and kidney-derived AR acid (KAR) were prepared by ammonium sulfate precipitation and centrifugation, respectively. The supernatant was collected, ammonium sulfate was added to 40% saturation, and the mixture was agitated for 30 min and centrifuged for 20 min at 10,000 r/min. The resulting supernatant was then treated with ammonium sulfate to 50% saturation, agitated for 30 min, and centrifuged again for 20 min at 10,000 r/min. The supernatant was further treated with ammonium sulfate to 75% saturation, agitated for 30 min, and centrifuged at 10,000 r/min. The resulting precipitate was collected, dissolved in 20 ml phosphate buffer, and dialyzed for 12 h in 4 L of the same buffer. The obtained crude enzyme was then aliquoted and frozen for storage. The crude enzyme solutions of the rat lens and kidney samples were prepared using the same method.

*Determination of protein content in crude enzyme AR:* The standard protein solutions were prepared at concentrations of 20, 40, 60, 80, and 100 μ/mL using bovine serum albumin as the standard protein. The absorbance was determined at 595 nm using the Coomassie Brilliant Blue method, and the protein content of crude enzyme was calculated.

The linear equation was y = 5.96 x-0.0438, r2 = 0.9904, and the content of crude enzyme protein was 37.55 mg/mL.

*Optimization of AR enzyme activity assay:* We optimized the method for measuring AR activity presented in previous studies on the effects of NADPH concentration, DL-glyceraldehyde concentration, AR enzyme content, and temperature on AR activity [20]. The optimized reaction system comprises 100 μL AR enzyme solution, 15.6 μmol/L NADPH, 10.0 mmol/L β-mercaptoethanol, 400 mmol/L lithium sulfate, 0.20 mmol/L DL glyceraldehyde, and 100 mmol/L pH 6.2 phosphate buffer. The optimum temperature of AR in the enzymatic reaction was 37°C.

*Studies on the effects of notoginseng saponins on LAR and KAR:* We studied each component's AR activity inhibition capabilities in the optimized conditions mentioned above. The total reaction system was 1 ml, containing 100 ml AR enzyme solution, 15.6 μmol NADPH, 10 mmol β-mercaptoethanol, 400 mmol lithium sulfate, 0.20 mmol DL glyceraldehyde, 0.1 mmol/L pH 6.2 phosphate buffer, and 100 μl of each component solution at different concentrations. Appropriate volumes of DMSO were added for components with poor water solubility, not exceeding 1% of the total reaction volume. The reaction was conducted at 37°C for 5 min, and the decrease in the optical density was assessed.

The AR inhibition rate of the samples was calculated as follows: inhibition rate (%) = [1-(A2-A0)/(A1-A0)] × 100% [21], where A0 represents the decrease in NADPH natural oxidation absorbance per minute without the enzyme, substrate, and sample; A1 represents the decrease in NADPH absorbance per minute for unadded samples; and A2 represents the decrease in NADPH absorbance per minute for added samples. The inhibition curves of each component were constructed with the sample concentration as the horizontal coordinate and the inhibition rate as the vertical coordinate.

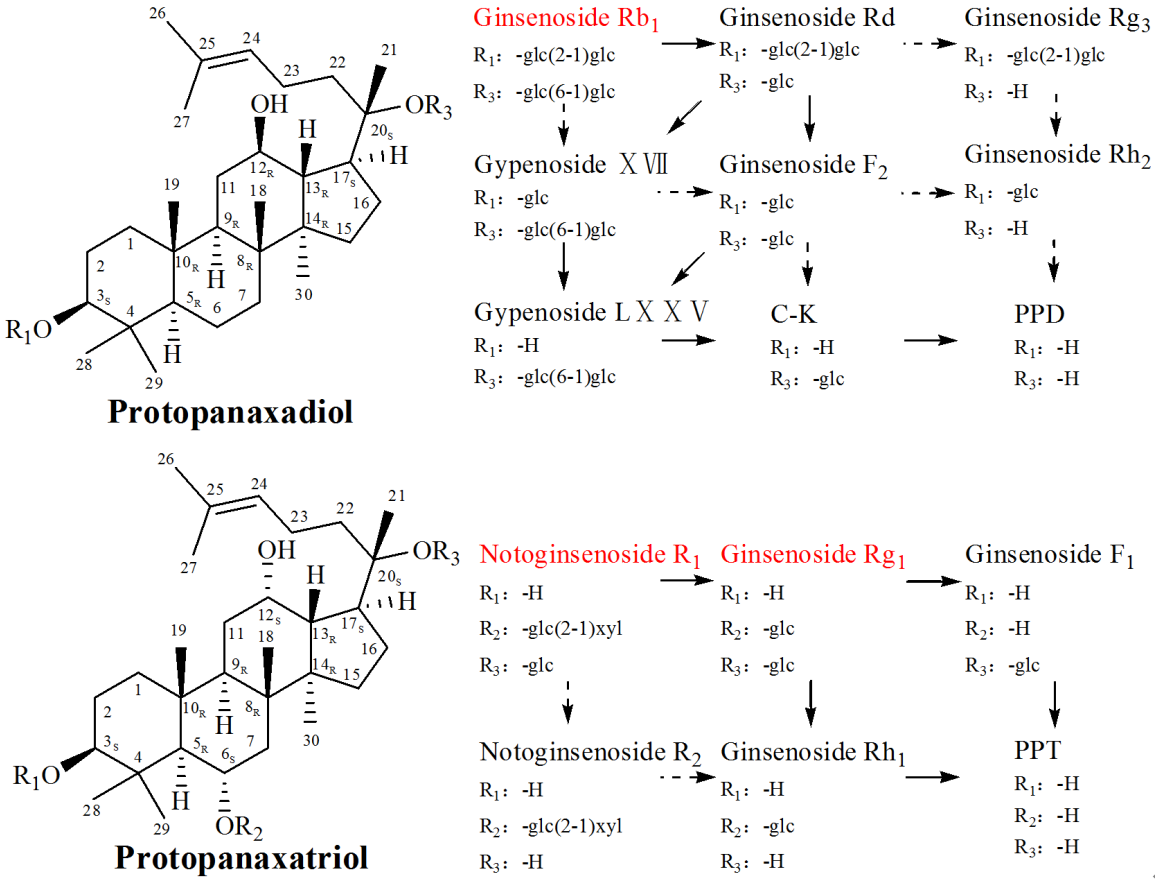


**Figure 1.** The included notoginsenosides according to their metabolism *in vivo*. The compounds shown in red font are the prototype Panax notoginseng saponins *in vivo*; those in black font were also included in this study.

*Data analysis*

SPSS 17.0 software was used for the data analysis. First, a single sample K-S test was used to test the normality of the data. An independent-samples *t* test was used for intergroup comparisons for data demonstrating a normal distribution. A nonparametric (Mann-Whitney U) test was used for non-normally distributed data. $P < 0.05$ was considered to indicate significance. The concentration inhibition rate curve was fitted using SPSS 17.0, and the AR inhibition rate was calculated.

## Results

*Molecular screening of the Panax notoginseng saponin*

*Prototype and metabolic components of Panax notoginseng saponins in vivo:* The main active ingredient in Panax notoginseng, Ginsenoside $Rb_1$, is a protopanaxadiol type dammarane type triterpenoid saponin, while Ginsenoside $R_1$ and Ginsenoside $Rg_1$ are protopanaxatriol type dammarane type tris-terpenoid saponins. Therefore, this study included three types of saponins, Ginsenoside $Rb_1$, Notoginsenoside $R_1$, and Ginsenoside $Rg_1$, as well as their *in vivo* metabolic components, as shown in **Figure 1**.

*Panax notoginseng saponin with different glycosyls:* To investigate whether the type of oxygen-containing glycosyl affects the biological effects of Panax notoginseng saponin, we included saponins with the same oxygen-containing glycosyl substitution positions but different glycosyl types in our Panax notoginseng saponin study as shown in **Figure 2**.

According to the above conditions, 23 compounds were selected, as shown in **Table 1** (ID: 1-23). We downloaded the physical and chemical parameters and CAS numbers from the CAS database. The ID 24 compound epalrestat was used as a positive control drug. Epalrestat is

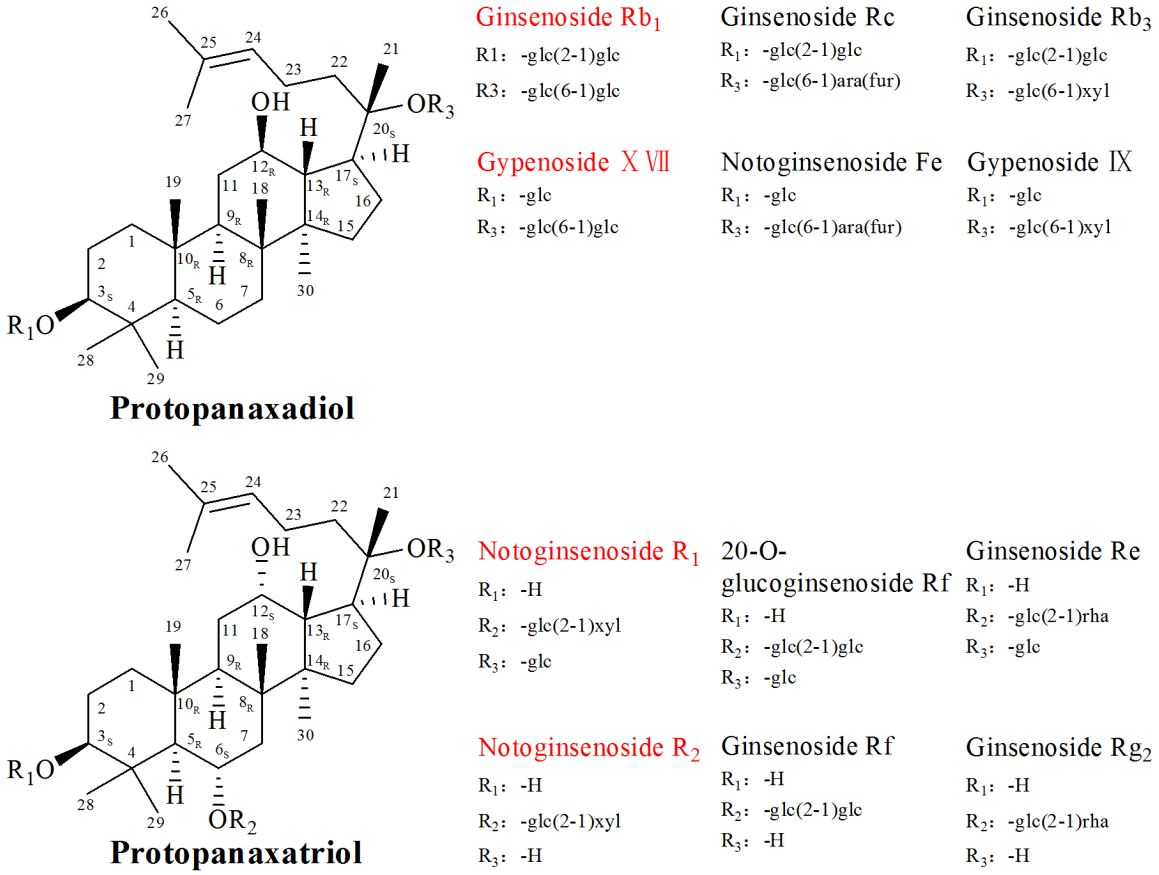


**Figure 2.** The included notoginsenosides according to the type of glycosyl in the structure. The compounds shown in red font were previously studied, and those shown in black font were newly incorporated in this study.

currently the only ARI in clinical use and has confirmed efficacy.

*Screening of Panax notoginseng saponins for AR inhibition capabilities via molecular binding assessment*

*Docking score:* Molecular docking is an important molecular simulation method that explores the recognition process between two or more molecules through computer simulation. The process involves complementary spatial morphology and energy matching between molecules. We used a scoring function to evaluate and infer the strength of molecular binding [22]. Molecular docking analysis was performed between AR and the 23 compounds, tolrestat, and epalrestat. The molecular docking scores were then calculated (**Table 2**). The docking score of compound ID 1-14 and AR was greater than that of the original ligand toristat and AR. The docking score of compound ID 16 (epalrestat) and AR was close to that of toristat (compound ID 15), indicating that compounds ID 1-14 and epalrestat successfully docked with AR. The docking score of compounds ID 17-25 could not be calculated, indicating that they failed to dock with AR or could not obtain a stable conformation after docking.

*Analysis of binding free energy and binding modes:* Binding free energy refers to the interaction between ligands and receptors and is an important indicator for measuring system stability. The system is stable when the binding free energy value is negative. The binding free energy values of the 16 compounds obtaining a stable conformation after docking with AR are shown in **Table 2** (arranged in descending order of binding free energy).

The stereoconformation, binding mode, binding site, and other information about the compounds binding to AR are shown in **Figure 3**.

**Table 1.** Libdock scores of compounds and aldose reductase

| ID | Compound | Libdock Score |
|---|---|---|
| 1 | Ginsenoside Rf | 166.248 |
| 2 | Notoginsenoside $R_2$ | 165.971 |
| 3 | Ginsenoside $F_2$ | 150.641 |
| 4 | Ginsenoside $Rh_1$ | 150.314 |
| 5 | Ginsenoside $Rh_2$ | 147.411 |
| 6 | Gypenoside LXXV | 142.878 |
| 7 | Ginsenoside $F_1$ | 139.852 |
| 8 | Ginsenoside $Rg_3$ | 127.714 |
| 9 | Ginsenoside C-K | 127.316 |
| 10 | Notoginsenoside Fe | 125.494 |
| 11 | Ginsenoside $Rg_2$ | 125.261 |
| 12 | Protopanaxatriol | 124.526 |
| 13 | Gypenoside IX | 122.874 |
| 14 | Protopanaxadiol | 121.859 |
| 15 | Tolrestat | 111.49 |
| 16 | Epalrestat | 110.18 |
| 17 | Gypenoside XVII | Uncomputable |
| 18 | Ginsenoside Rd | Uncomputable |
| 19 | Ginsenoside $Rb_1$ | Uncomputable |
| 20 | Ginsenoside Rc | Uncomputable |
| 21 | Ginsenoside $Rb_3$ | Uncomputable |
| 22 | Ginsenoside $Rg_1$ | Uncomputable |
| 23 | 20-O-glucoginsenoside Rf | Uncomputable |
| 24 | Ginsenoside Re | Uncomputable |
| 25 | Notoginsenoside $R_1$ | Uncomputable |

Epalrestat, an ARI used in clinical practice, undergoes electrostatic interactions with HIS-110, forms hydrogen bonds with amino acid residues TYR48, LYS77, HIS110, TRP111, ASN-160, and GLN183, and forms hydrophobic interactions with TRP20, VAL47, PHE122, and LEU300. Epalrestat also exhibits p- π conjugation effects with HIS110 and TRP111. Tolrestat forms hydrogen bonds with amino acid residues TYR48, TRP111, and THR113, forms hydrophobic interactions with TRP111 and LEU300, and exhibits p- π conjugation with TYR48. This finding aligns with previous studies indicating that TYR48 and TRP111 are key amino acids that bind epalrestat, tolrestat, and AR, with hydrogen bonding interactions representing the primary type of action [23-25].

**Figure 4** shows the stereoconformations of Ginsenoside $Rg_2$, Notoginsenoside $R_2$, Ginsenoside Rf, Ginsenoside $F_2$, Gypenoside IX, Ginsenoside $F_1$, and Ginsenoside $Rh_2$ in complex with aldose reductase. The stereoconformations and related information of other compounds binding to AR can be found in **Appendix A**.

**Table 2.** Binding free energy of compounds and aldose reductase

| NO. | ID | Compound | Binding Free Energy |
|---|---|---|---|
| 1 | 16 | Epalrestat | -199.453 |
| 2 | 15 | Tolrestat | -164.127 |
| 3 | 11 | Ginsenoside $Rg_2$ | -133.313 |
| 4 | 2 | Notoginsenoside $R_2$ | -79.91 |
| 5 | 1 | Ginsenoside Rf | -73.818 |
| 6 | 3 | Ginsenoside $F_2$ | -64.065 |
| 7 | 13 | Gypenoside IX | -60.796 |
| 8 | 7 | Ginsenoside $F_1$ | -57.076 |
| 9 | 5 | Ginsenoside $Rh_2$ | -53.419 |
| 10 | 6 | Gypenoside LXXV | -46.704 |
| 11 | 9 | Ginsenoside C-K | -44.076 |
| 12 | 8 | Ginsenoside $Rg_3$ | -18.078 |
| 13 | 14 | Protopanaxadiol | -13.565 |
| 14 | 10 | Notoginsenoside Fe | 8.509 |
| 15 | 12 | Protopanaxatriol | 11.595 |
| 16 | 4 | Ginsenoside $Rh_1$ | 38.351 |

Ginsenoside $Rg_2$ forms hydrogen bonds with amino acid residues TRP20, VAL47, GLN49, TRP111, and SER302, and forms hydrophobic interactions with TRP20, LYS21, VAL47, TYR48, TRP79, TRP111, PHE122, TRP219, CYS298, and LEU300. Notoginsenoside $R_2$ forms hydrogen bonds with amino acid residues TYR48, HIS110, CYS298, and SER302, and forms hydrophobic interactions with PHE122 and TRP219. Ginsenoside Rf forms hydrogen bonds with amino acid residues HIS110, TRP111, and SER302, and forms hydrophobic interactions with TRP20, PRO23, PRO24, VAL47, TYR48, TRP79, TRP111, PHE122, PRO218, TRP219, CYS298, and LEU300. Ginsenoside $F_2$ forms hydrogen bonds with amino acid residues TRP111, GLN183, SER210, and PRO218, and forms hydrophobic interactions with TRP20, VAL47, TYR48, TRP79, HIS110, TRP111, PHE122, TRP219, and LEU300. Gypenoside IX forms hydrogen bonds with amino acid residues TRP20, VAL47, TYR48, TRP111, GLN183, and SER210, and forms hydrophobic interactions with TRP20, VAL47, TYR48, TRP79, HIS110, TRP111, PHE122, LEU124, TRP219,

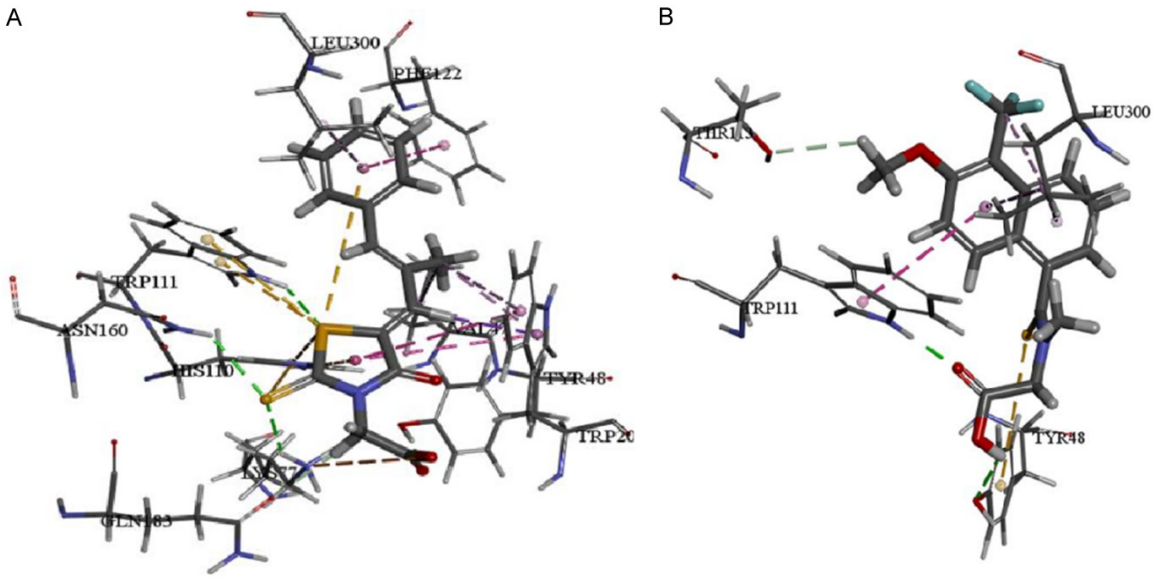


**Figure 3.** Molecular interactions of epalrestat and tolrestat with aldose reductase. A. Molecular interactions of epalrestat with aldose reductase; B. Molecular interactions of tolrestat with aldose reductase.

CYS298, and LEU300. Ginsenoside $F_1$ forms hydrogen bonds with amino acid residues TRY48, TRP111, and SER159, and forms hydrophobic interactions with TRP20, VAL47, TRP79, HIS110, TRP111, PHE115, PHE122, VAL130, PRO218, LEU300, and CYS303.

*Effect of Panax notoginseng saponins on LAR*

We randomly selected Ginsenoside Rf, Ginsenoside $F_1$, Ginsenoside C-K, and Ginsenoside $Rh_1$ from the 14 compounds of Panax notoginseng saponins that successfully docked with AR and obtained stable conformations after docking. Furthermore, we selected Notoginsenoside $R_1$, for which a docking score could not be calculated, and epalrestat, a clinically used ARI. Subsequently, we performed *in vitro* experimental studies on the inhibition rate of LAR. The inhibition curves of each component were plotted with compound concentration on the x-axis and inhibition rate on the y-axis, as shown in **Figure 5**.

The inhibition rate of epalrestat on LAR *in vitro* increases with increasing concentration. When the concentration of epalrestat reaches 1 μM, the inhibition rate tends to stabilize with increasing concentration, reaching 80% to 90%. Notoginsenoside $R_1$ (B1) did not significantly affect LAR activity in the measured concentration range. When the concentration of Ginsenoside Rf (C1), Ginsenoside $Rh_1$ (D1), and Ginsenoside $F_1$ (E1) in the system is 50 μM, they exhibit LAR activation activity with activation rates of 15.8%, 2.4%, and 8.8%, respectively. As the concentration in the system decreases, the excitatory activity decreases and gradually produces an inhibitory effect. The inhibitory effect is greatest when the concentration in the system is 3.1-6.3 μM, with inhibition rates of 9.5%, 6.4%, and 5.1% for the three compounds, respectively. As the concentration in the system further decreases, the inhibitory effect decreases until there is no significant inhibitory or excitatory effect. When the concentration of Ginsenoside CK (F1) in the system is 50 μM, it exhibits a weak inhibitory effect with an inhibition rate of 7.3%. As the concentration in the system decreases, the inhibitory activity gradually increases. The maximum inhibitory effect is 26.8% at a concentration of 6.3 μM. As the concentration in the system further decreases, its inhibitory effect decreases until no significant inhibition occurs.

*The effect of Panax notoginseng saponins on KAR*

Ginsenoside Rf, Ginsenoside $F_1$, Ginsenoside C-K, Ginsenoside $Rh_1$, Notoginsenoside $R_1$, and epalrestat were selected for experimental studies of the rate of KAR inhibition *in vitro*. The inhibition curves of each component were plot-

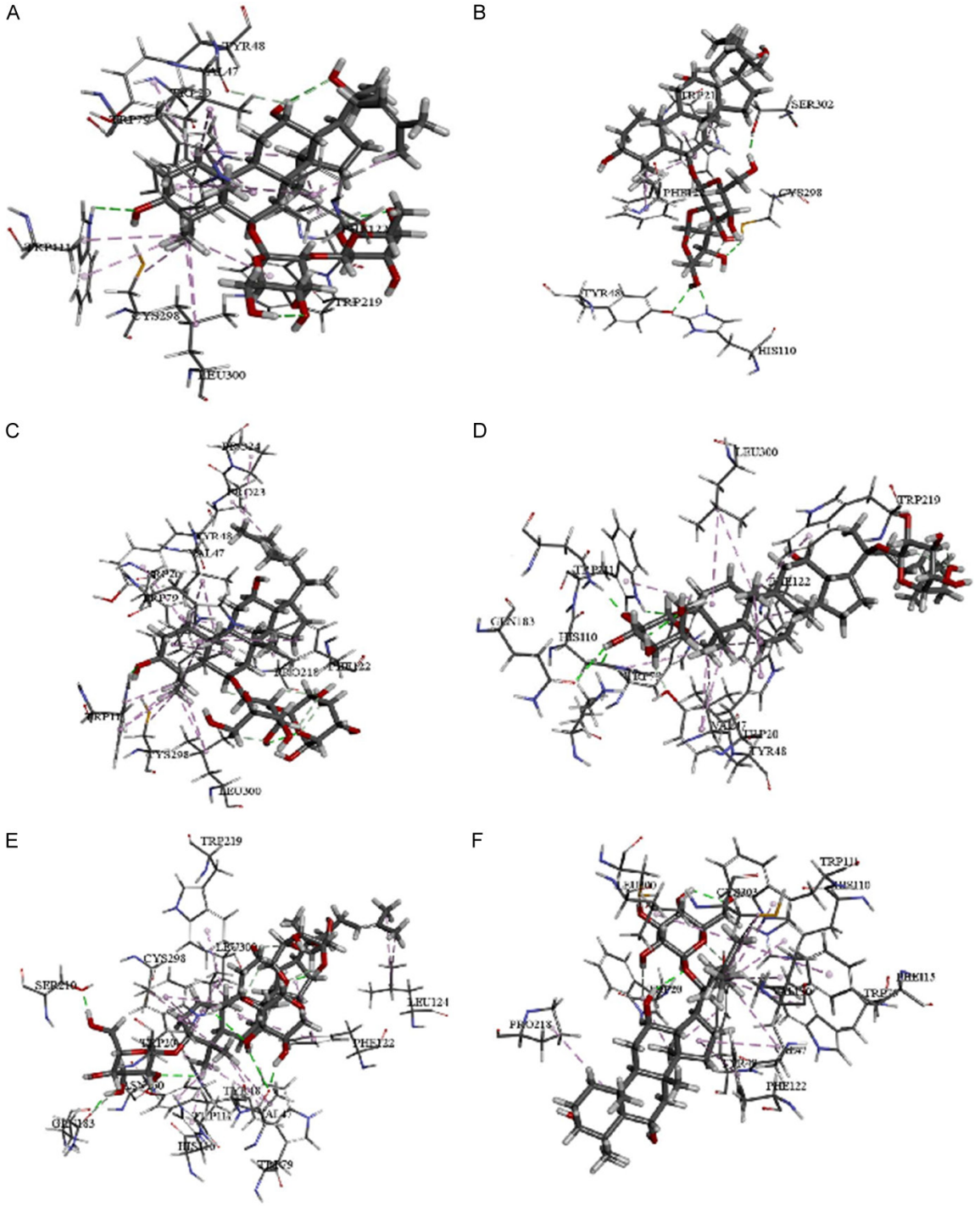


**Figure 4.** Molecular interactions with aldose reductase. A. Ginsenoside $Rg_2$; B. Notoginsenoside $R_2$; C. Ginsenoside Rf; D. Ginsenoside $F_2$; E. Gypenoside IX; F. Ginsenoside $F_1$.

ted with compound concentration on the x-axis and inhibition rate on the y-axis, as shown in **Figure 6**.

The inhibition rate of epalrestat on KAR *in vitro* increases with increasing concentration. When the concentration of epalrestat reaches 1 μM, the inhibition rate tends to stabilize with increasing concentrations, reaching 80%-90%. Notoginsenoside $R_1$ (B2) has no significant effect on the activity of KAR within the determined concentration range. When the concen-

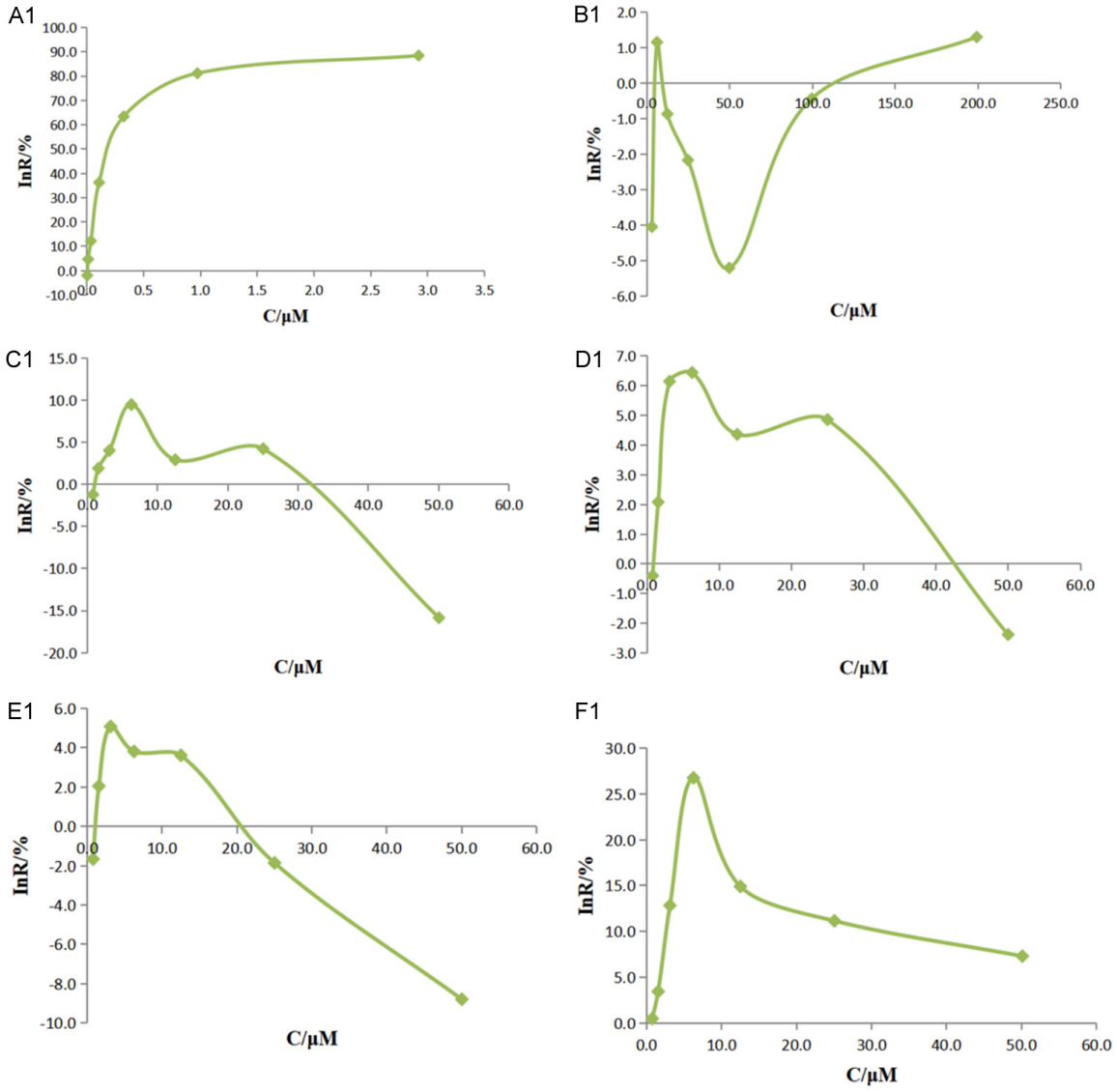


**Figure 5.** Concentration-inhibition rate curve of lens aldose reductase for each compound. A1. Eparestat; B1. Notoginsenoside $R_1$; C1. Ginsenoside Rf; D1. Ginsenoside $Rh_1$; E1. Ginsenoside $F_1$; F1. Ginsenoside CK.

tration of Ginsenoside Rf (C2), Ginsenoside $Rh_1$ (D2), and Ginsenoside $F_1$ (E2) in the system is 50 μM, they exhibit KAR activation activity, with activation rates of 22.0%, 6.1%, and 11.9%, respectively. As the concentration in the system decreases, the excitatory activity decreases and gradually yields an inhibitory effect. The inhibitory effect is greatest when the concentration in the system is 3.1-6.3 μM, yielding 8.4%, 7.2%, and 7.2% across the three compounds, respectively. As the concentration in the system further decreases, the inhibitory effect decreases until no significant inhibitory or excitatory effect is observed. When the concentration of Ginsenoside CK (F2) in the system is 50 μM, it exhibits a weak inhibitory effect with an inhibition rate of 7.5%. As the concentration in the system decreases, the activity gradually increases, and the maximum inhibition rate is 33.0% when the concentration in the system is 6.3 μM. As the concentration in the system further decreases, its inhibitory effect decreases until no significant inhibitory or excitatory effect is observed.

## Discussion

DM is a prevalent metabolic disorder, and its complications, such as diabetic retinopathy and nephropathy, significantly compromise

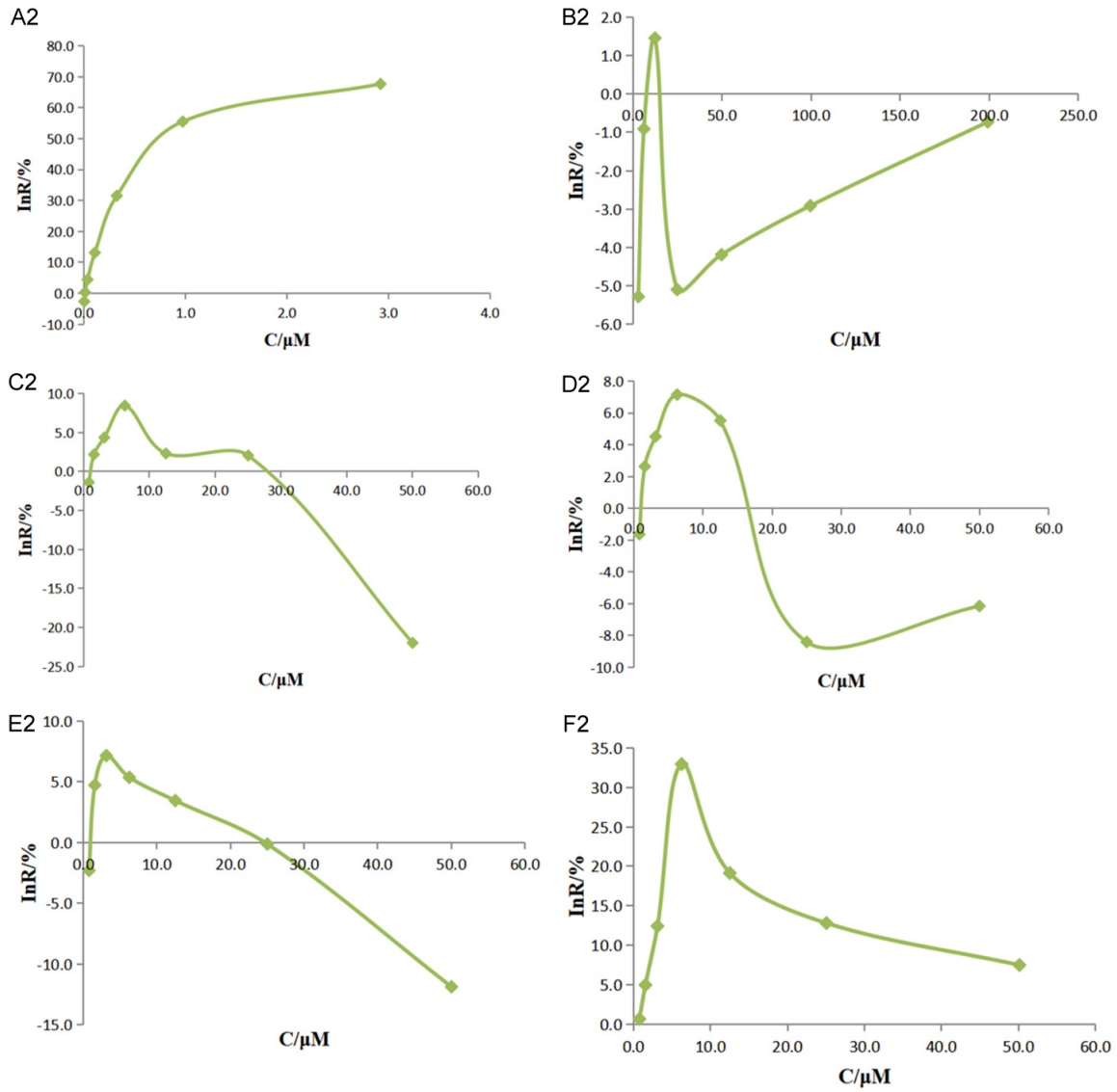


**Figure 6.** Concentration-inhibition rate curve of kidney aldose reductase for each compound. A2. Eparestat; B2. Notoginsenoside $R_1$; C2. Ginsenoside Rf; D2. Ginsenoside $Rh_1$; E2. Ginsenoside $F_1$; F2. Ginsenoside CK.

patients' quality of life. ARIs have emerged as a potential therapeutic approach for managing these complications. However, the development and clinical application of ARIs is challenging. Currently, only epalrestat is used clinically in some regions, and no ARI has been globally approved by the FDA. The limited clinical use of ARIs is mainly attributable to their poor enzyme specificity. ARIs not only inhibit AR but also significantly affect aldehyde reductase (ALR), an isoenzyme in the aldehyde-ketone reduction family responsible for detoxifying harmful aldehydes and ketones. This dual inhibition effect can lead to adverse reactions [26].

In this study, we investigated the effects of Panax notoginseng saponins on AR. Our results demonstrated a bidirectional regulatory effect of Panax notoginseng saponins on the activity of LAR and KAR. This finding is distinct from those reported in numerous previous studies, in which a unidirectional effect on enzyme activity was observed with these compounds [27]. For example, some traditional ARIs were designed to solely inhibit AR activity. The bidirectional regulation we observed implies a more complex interaction mechanism between Panax notoginseng saponins and AR.

The bidirectional nature of the selected monomeric saponin compounds' effects on LAR/

KAR is related to their water solubility and concentration in the system. Monomeric saponins with good water solubility exhibit inhibitory effects at high concentrations and excitatory effects at low concentrations, while the opposite is true for poorly water-soluble monomeric saponins. This phenomenon might be explained by the different ways in which these saponins interact with the enzyme's active site. Highly soluble saponins may saturate the active site at high concentrations, leading to inhibition, while at low concentrations, they may bind in a way that promotes enzyme activity. Poorly water-soluble saponins' aggregation behavior at high concentrations might facilitate interactions that activate the enzyme, and at low concentrations, they may bind more specifically to inhibitory sites.

Moreover, the experimental results suggest differences in the binding mode and strength when this type of compound is coincubated with AR in different proportions. This finding is consistent with the complexity of the interaction between natural compounds and enzymes. Furthermore, this finding indicates that the single-molecule docking method used in this study has limitations. Previous studies relying solely on single-molecule docking might have overlooked the dynamic and multimolecular nature of these interactions. In the future, multi-molecule docking methods should be explored to better understand the binding mechanism between Panax notoginseng saponins and AR.

Comparing our results with previous studies on Panax notoginseng saponins, most prior research focused on their effects on blood circulation, hemostasis, and the cardiovascular system [28, 29]. While some studies have hinted at the potential role of these saponins in diabetes treatment, the specific mechanism related to AR inhibition or regulation has not been well-explored. Our study fills this gap by directly investigating the interaction between Panax notoginseng saponins and AR.

However, this study has several limitations. First, the experiments were mainly conducted *in vitro*, and the results may not fully represent the situation *in vivo*. The complex physiological environment in the body, including the presence of other proteins, hormones, and metabolic pathways, could influence the interaction between Panax notoginseng saponins and AR. Second, we only studied a limited number of Panax notoginseng saponin monomers. There are numerous other saponin components in Panax notoginseng, and their effects on AR remain unknown. Third, we used single-molecule docking, which may not accurately reflect the real-world binding scenario.

Several directions can be considered for future research. *In vivo* animal experiments should be conducted to confirm the bidirectional regulatory effect of Panax notoginseng saponins on AR and to explore its impact on diabetes complications in an *in vivo* model. A comprehensive study on all saponin components of Panax notoginseng is needed to fully understand their potential as ARIs. Additionally, advanced techniques such as multimolecule docking, molecular dynamics simulations, and *in vivo* imaging should be employed to precisely elucidate the binding mechanism between Panax notoginseng saponins and AR at the molecular level. These studies will provide a more solid foundation for the development of novel and effective ARIs based on Panax notoginseng saponins.

## Conclusion

The results suggest that the binding of monomeric saponin components to LAR/KAR may involve a multimolecular mechanism. When LAR/KAR and monomeric saponin compounds are coincubated at different molecular ratios, their binding sites, modes, and strengths may differ, resulting in differences in biological activity, such as activation or inhibition. However, this biological activity is not selective for the activity of LAR and KAR. The significance of this study lies in establishing a stable and reproducible method for preparing AR crude enzymes and an enzyme activity evaluation system. This system enabled an observation of the bidirectional regulatory effect of Panax notoginseng saponins on LAR and KAR activities, providing new ideas for investigating saponin activity in the context of AR activity regulation.

## Acknowledgements

We thank LetPub (www.letpub.com.cn) for its linguistic assistance during the preparation of this manuscript. This research was supported by the Beijing Natural Science Foundation, No. 7254488, and Major Science and Technology Projects of Beijing Polytechnic, grant number 2024X005-KXD.

## Disclosure of conflict of interest

None.

**Address correspondence to:** Dr. Wen-Ting Fei, School of Bioengineering, Beijing Polytechnic University, No. 9 Liangshuihe 1st Street, Beijing Economic and Technological Development Zone, Beijing, China. E-mail: feiwenting@bpi.edu.cn

## References

[1] Whiting DR, Guariguata L, Weil C and Shaw J. IDF diabetes atlas: global estimates of the prevalence of diabetes for 2011 and 2030. Diabetes Res Clin Pract 2011; 94: 311-321.

[2] Alexiou P, Pegklidou K, Chatzopoulou M, Nicolaou I and Demopoulos VJ. Aldose reductase enzyme and its implication to major health problems of the 21(st) century. Curr Med Chem 2009; 16: 734-752.

[3] Yabe-Nishimura C. Aldose reductase in glucose toxicity: a potential target for the prevention of diabetic complications. Pharmacol Rev 1998; 50: 21-33.

[4] Kao YL, Donaghue K, Chan A, Knight J and Silink M. A novel polymorphism in the aldose reductase gene promoter region is strongly associated with diabetic retinopathy in adolescents with type 1 diabetes. Diabetes 1999; 48: 1338-1340.

[5] Srinivasan V, HyeLim N, Radha A, Ni Son, Kellie H, Yunying H, Shuiquing Y, Xiaoping S, Rosa R, Yan L, Thyyar R, Konstantinos D, Lesley AH, Ann MS, Ira JG and Ravichandran R. Human aldose reductase expression accelerates atherosclerosis in diabetic apolipoprotein E-/- mice. Arterioscler Thromb Vasc Biol 2011; 31: 1805-1813.

[6] Milan S, Vladimir S, Paul-Omer D, Magdalena M, Vassilis D, Lucia R, Zelmira B, Cimen K, Vincenzo C and Ossama El. Carboxymethylated pyridoindole antioxidants as aldose reductase inhibitors: synthesis, activity, partitioning, and molecular modeling. Bioorg Med Chem 2008; 16: 4908-4920.

[7] Liu XJ, Hu XK, Yang H, Gui LM, Cai ZX, Qi MS and Dai CM. A review of traditional chinese medicine on treatment of diabetic nephropathy and the involved mechanisms. Am J Chin Med 2022; 50: 1739-1779.

[8] An X, Xu Y and Gui D. Combination of astragalus membranaceus and panax notoginseng as main components in the treatment of diabetic nephropathy: a systematic review and meta-analysis. Evid Based Complement Alternat Med 2023; 2023: 2945234.

[9] Mi W, Yu M, Yin S, Ji Y, Shi T and Li N. Analysis of the renal protection and antioxidative stress effects of panax notoginseng saponins in diabetic nephropathy mice. J Immunol Res 2022; 2022: 3610935.

[10] Wang Y, Sun X, Xie Y, Du A, Chen M, Lai S, Wei X, Ji L and Wang C. Panax notoginseng saponins alleviate diabetic retinopathy by inhibiting retinal inflammation: association with the NF-κB signaling pathway. J Ethnopharmacol 2024; 319: 117135.

[11] Wu F, Lai S, Fu D, Liu J, Wang C, Feng H, Liu J, Li Z and Li P. Neuroprotective effects and metabolomics study of protopanaxatriol (PPT) on cerebral ischemia/reperfusion injury *in vitro* and *in vivo*. Int J Mol Sci 2023; 24: 1789.

[12] Pang HH, Li MY, Wang Y, Tang MK, Ma CH and Huang JM. Effect of compatible herbs on the pharmacokinetics of effective components of Panax notoginseng in Fufang Xueshuantong Capsule. J Zhejiang Univ Sci B 2017; 18: 343-352.

[13] Li CT, Wang HB and Xu BJ. A comparative study on anticoagulant activities of three Chinese herbal medicines from the genus Panax and anticoagulant activities of ginsenosides Rg1 and Rg2. Pharm Biol 2013; 51: 1077-1080.

[14] Liu R, Qin M, Hang P, Liu Y, Zhang Z and Liu G. Effects of Panax notoginseng saponins on the activities of CYP1A2, CYP2C9, CYP2D6 and CYP3A4 in rats *in vivo*. Phytother Res 2012; 26: 1113-1118.

[15] Zheng H, Liu C, Ou Y, Zhang Y and Fu X. Total saponins of Panax notoginseng enhance VEGF and relative receptors signals and promote angiogenesis derived from rat bone marrow mesenchymal stem cells. J Ethnopharmacol 2013; 147: 595-602.

[16] He NW, Zhao Y, Guo L, Shang J and Yang XB. Antioxidant, antiproliferative, and pro-apoptotic activities of a saponin extract derived from the roots of Panax notoginseng (Burk.) F.H. Chen. J Med Food 2012; 15: 350-359.

[17] Chen ZH, Li J, Liu J, Zhao Y, Zhang P, Zhang MX and Zhang L. Saponins isolated from the root of Panax notoginseng showed significant antidiabetic effects in KK-Ay mice. Am J Chin Med 2008; 36: 939-951.

[18] Zhao L, Lan LG, Min XL, Lu AH, Zhu LQ, He XH and He LJ. Integrated treatment of traditional Chinese medicine and western medicine for early- and intermediate-stage diabetic nephropathy. Nan Fang Yi Ke Da Xue Xue Bao 2007; 27: 1052-1055.

[19] Yamagishi S, Matsui T, Nakamura K, Ueda S, Noda Y and Imaizumi T. Pigment epithelium-derived factor (PEDF): its potential therapeutic implication in diabetic vascular complications. Curr Drug Targets 2008; 9: 1025-1029.

[20] Yang LH, Tang MK, Liu J and Huang JM. Inhibitory effects of major components of fufang xueshuantong capsule on aldose reductase.

China Journal of Traditional Chinese Medicine and Pharmacy 2015; 30: 586-589.
[21] Zhang H, Zhao T, Gong Y, Dong X, Zhang W, Sun S, Wang H, Gu Y, Lu X, Yan M and Li P. Attenuation of diabetic nephropathy by Chaihuang-Yishen granule through anti-inflammatory mechanism in streptozotocin-induced rat model of diabetics. J Ethnopharmacol 2014; 151: 556-564.
[22] Dong R, Huang R, Shi X, Xu Z and Mang J. Exploration of the mechanism of luteolin against ischemic stroke based on network pharmacology, molecular docking and experimental verification. Bioengineered 2021; 12: 12274-12293.
[23] Lee YS, Sugiyama K and Kador PF. Rotamers of tolrestat and their binding mode to aldose reductase. Adv Exp Med Biol 1999; 463: 465-472.
[24] Reddy TN, Ravinder M, Bagul P, Ravikanti K, Bagul C, Nanubolu JB, Srinivas K, Banerjee SK and Rao VJ. Synthesis and biological evaluation of new epalrestat analogues as aldose reductase inhibitors (ARIs). Eur J Med Chem 2014; 71: 53-66.
[25] Lee YS, Hodoscek M, Kador PF and Sugiyama K. Hydrogen bonding interactions between aldose reductase complexed with NADP(H) and inhibitor tolrestat studied by molecular dynamics simulations and binding assay. Chem Biol Interact 2003; 143-144: 307-16.
[26] Sapna T, Sonu KG, Villayat A, Priyanka S and Malkhey V. Aldose Reductase: a cause and a potential target for the treatment of diabetic complications. Arch Pharm Res 2021; 44: 655-667.
[27] Liu J, Wang Y, Qiu L, Yu Y and Wang C. Saponins of Panax notoginseng: chemistry, cellular targets and therapeutic opportunities in cardiovascular diseases. Expert Opin Investig Drugs 2014; 23: 523-539.
[28] Jian W, Yu S, Tang M, Duan H and Huang J. A combination of the main constituents of Fufang Xueshuantong Capsules shows protective effects against streptozotocin-induced retinal lesions in rats. J Ethnopharmacol 2016; 182: 50-56.
[29] Xu DD, Pang HH, Jiang MF, Jian WJ, Wang QH, Sun L, Dong ZY, Huang JM. LC-LTQ-Orbitrap analysis on chemical constituents in Scrophulariae Radix extract and their metabolites in rat plasma. Zhongguo Zhong Yao Za Zhi 2016; 41: 521-527.

# Appendix A

The stereoconformation, binding mode, binding site, and other information of the compounds of Ginsenoside $Rh_2$, Gypenoside LXXV, Ginsenoside C-K, Ginsenoside $Rg_3$, Protopanaxadiol, Notoginsenoside Fe, Protopanaxatriol, and Ginsenoside $Rh_1$ binding to aldose reductase are shown below.

Ginsenoside $Rh_2$ forms hydrogen bonds with the amino acid residue TRP20 and forms hydrophobic interactions with TRP20, HIS110, TRP111, PHE122, TYR209, PRO218, TRP219, and CYS298, as shown in **Figure 7**.

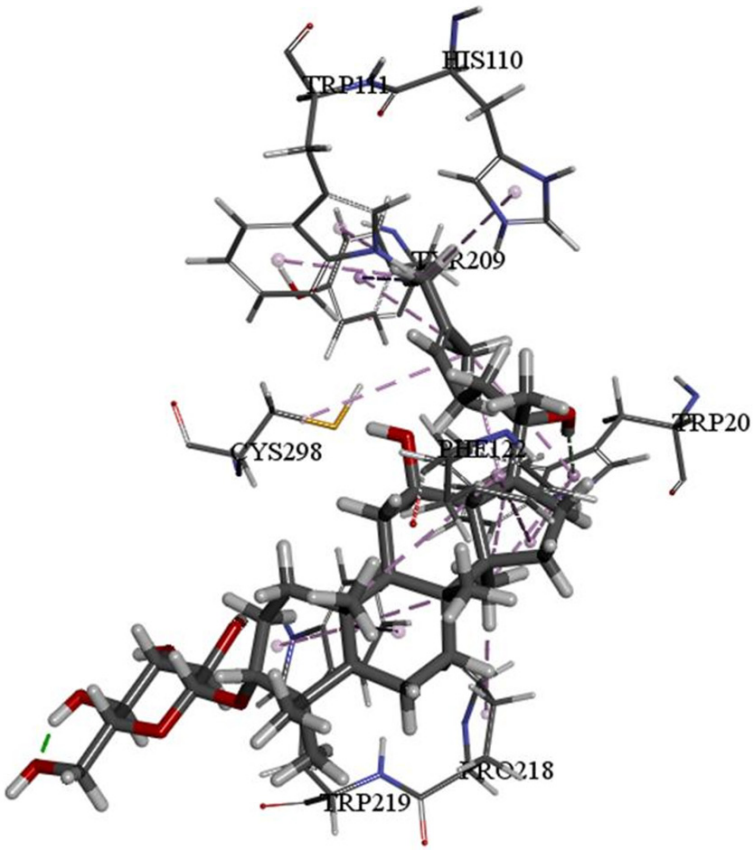


**Figure 7.** Molecular interactions of Ginsenoside $Rh_2$ with aldose reductase.

Gypenoside LXXV forms hydrogen bonds with amino acid residues LEU300, LEU301, and SER302 and forms hydrophobic interactions with TRP20, VAL47, TRP79, HIS110, PHE122, PRO218, TRP219, and LEU300, as shown in **Figure 8**.

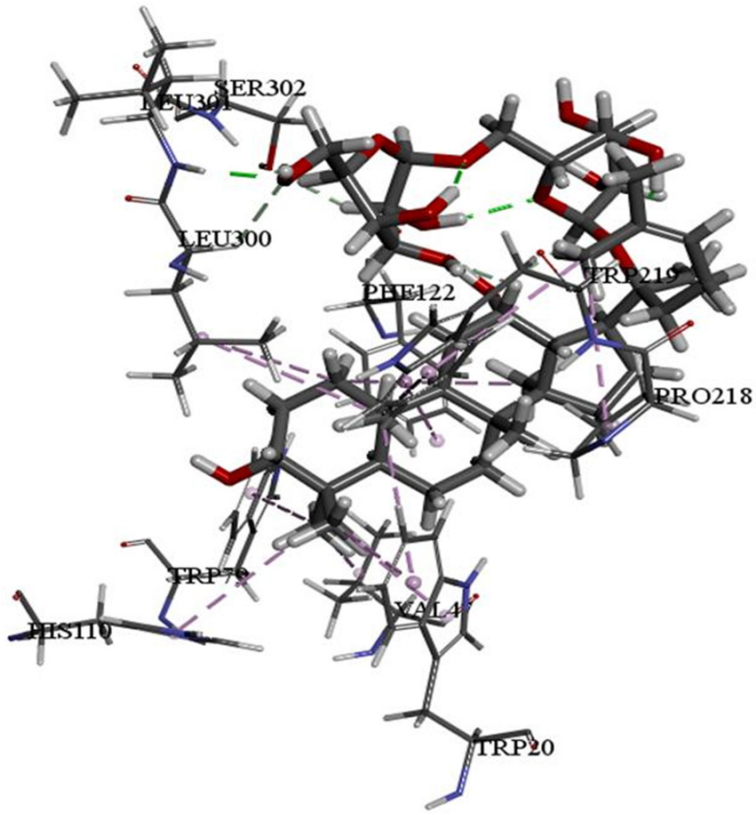


**Figure 8.** Molecular interactions of Gypenoside LXXV with aldose reductase.

Ginsenoside CK forms hydrogen bonds with the amino acid residue TRP20 and forms hydrophobic interactions with TRP20, VAL47, HIS110, TRP111, PHE122, TYR209, PRO218, TRP219, and CYS298, as shown in **Figure 9**.

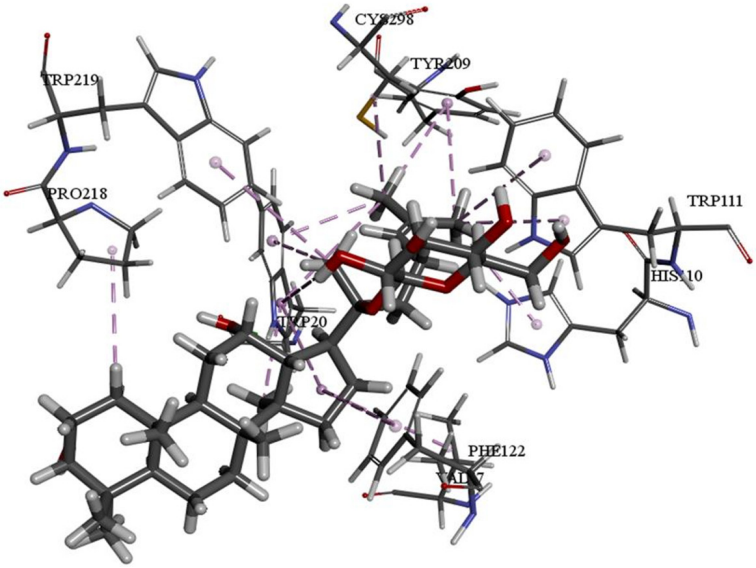


**Figure 9.** Molecular interactions of Ginsenoside C-K with aldose reductase.

Ginsenoside $Rg_3$ forms hydrogen bonds with amino acid residues TRP20 and PRO218 and forms hydrophobic interactions with TRP20, TRP79, TRP111, PHE122, TYR209, PRO218, TRP219, CYS298, and LEU300. Ginsenoside $Rg_3$ also undergoes p- π conjugation with TRP20, as shown in **Figure 10**.

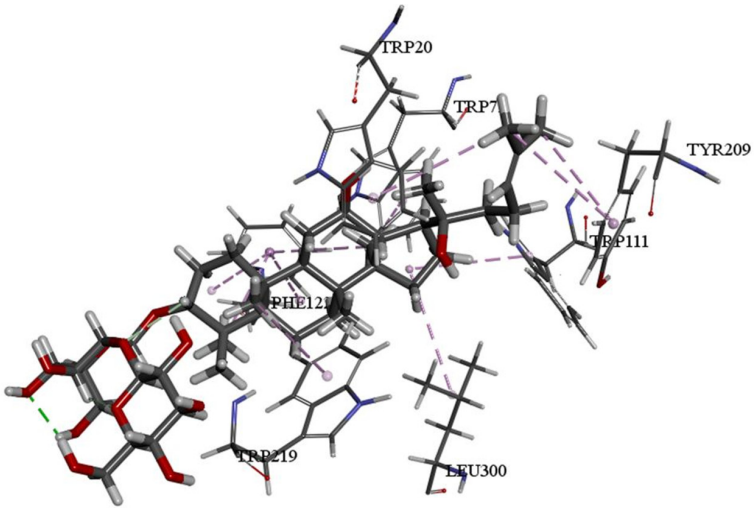


**Figure 10.** Molecular interactions of Ginsenoside $Rg_3$ with aldose reductase.

Protopanaxadiol forms hydrogen bonds with amino acid residues TRP20, TYR48, and HIS110 and forms hydrophobic interactions with TRP20, TRP79, TRP111, PHE122, TYR209, PRO218, ILE260, CYS298, and LEU300, as shown in **Figure 11**.

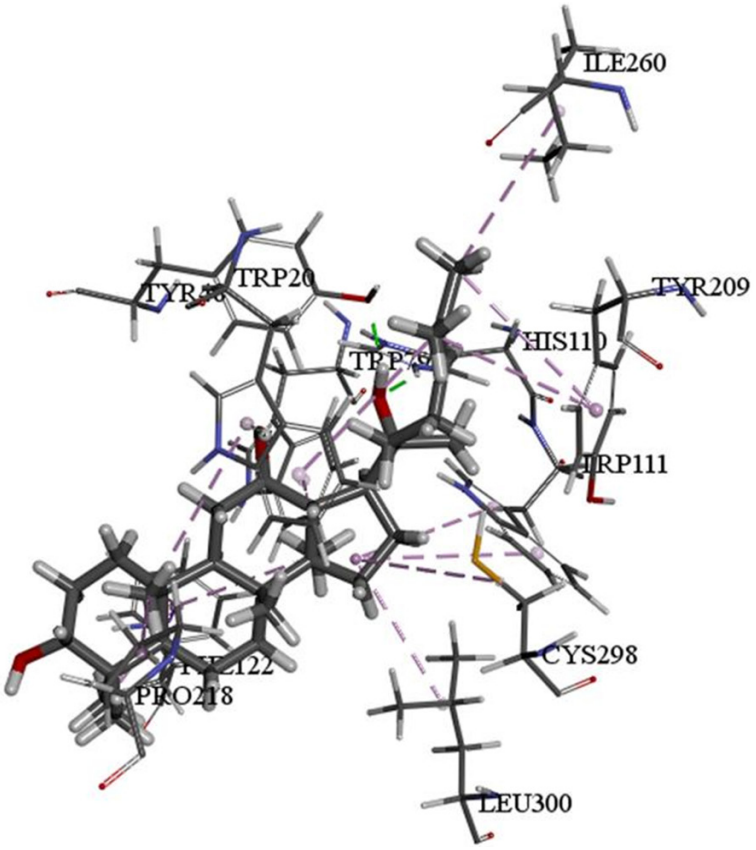


**Figure 11.** Molecular interactions of Protopanaxadiol with aldose reductase.

Notoginsenoside Fe forms hydrogen bonds with amino acid residues TYR48, PRO218, and SER302 and forms hydrophobic interactions with TRP20, VAL47, PHE122, LEU124, TRP219, and LEU300, as shown in **Figure 12**.

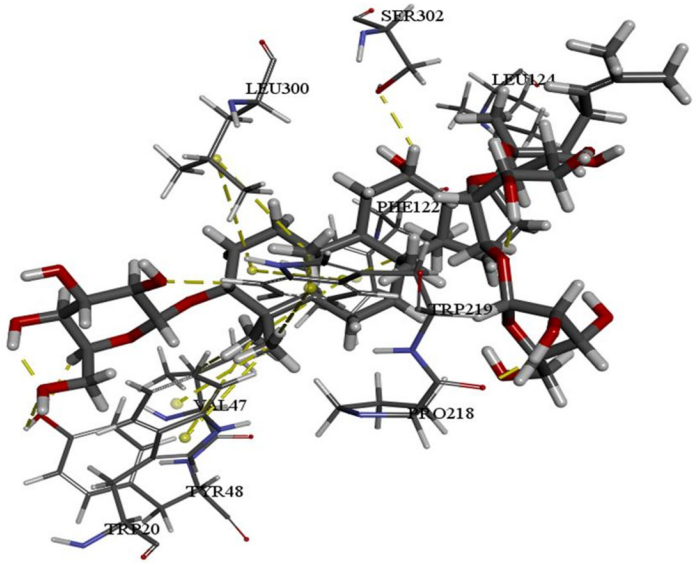


**Figure 12.** Molecular interactions of Notoginsenoside Fe with aldose reductase.

Protopanaxatriol forms hydrogen bonds with amino acid residues TYR48 and HIS110 and forms hydrophobic interactions with TRP20, TRP79, TRP111, PHE122, TYR209, ILE260, CYS298, and LEU300, as shown in **Figure 13**.

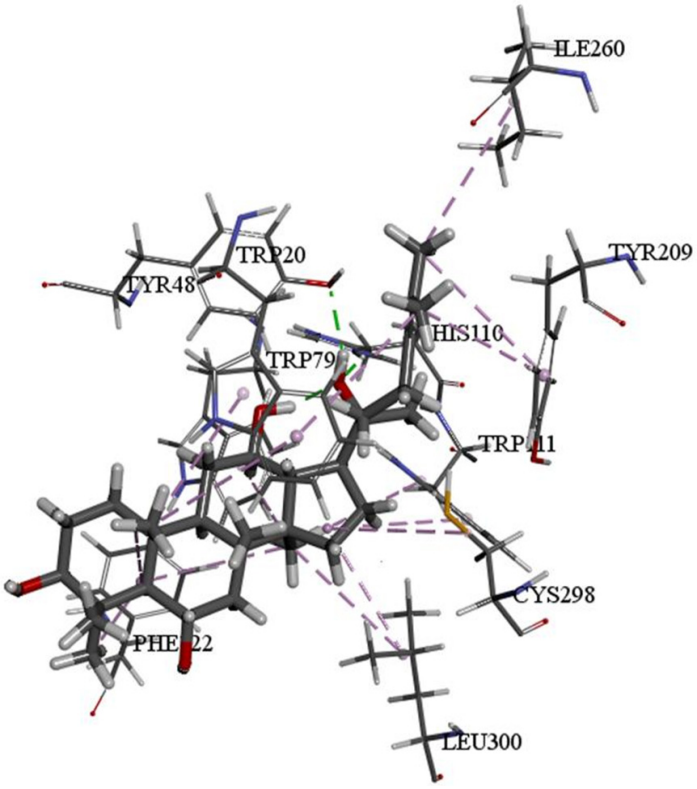


**Figure 13.** Molecular interactions of Protopanaxatriol with aldose reductase.

Ginsenoside $Rh_1$ forms hydrogen bonds with the amino acid residue Ser302 and forms hydrophobic interactions with TRP20, TRP79, PHE122, TYR209, PRO218, TRP219, and LEU300, as shown in **Figure 14**.

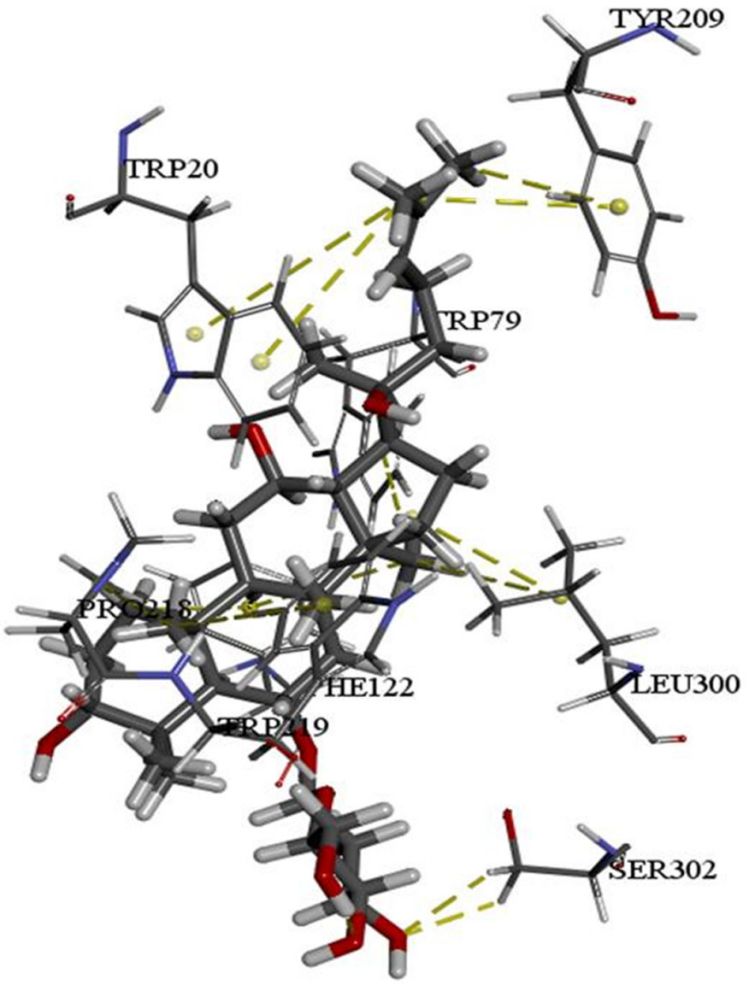


**Figure 14.** Molecular interactions of Ginsenoside $Rh_1$ with aldose reductase.